Preparation and Characterization of Highly Cross-Linked Polyimide Aerogels Based on Polyimide Containing Trimethoxysilane Side Groups

Xueliang Pei, Wentao Zhai, and Wenge Zheng*

Polymers and Composites Division, Ningbo Institute of Material Technology and Engineering, Chinese Academy of Sciences, Ningbo, Zhejiang 315201, PR China

Supporting Information

ABSTRACT: In this study, highly cross-linked and completely imidized polyimide aerogels were prepared from polyimide containing trimethoxysilane side groups, which was obtained as the condensation product of polyimide containing acid chloride side groups and 3-aminopropyltrimethoxysilane. After adding water and acid catalyst, the trimethoxysilane side groups hydrolyzed and condensed one another, and a continuous increase in the complex viscosities of the polyimide solutions with time was observed. The formed polyimide gels were dried by freeze-drying from *tert*-butyl alcohol to obtain polyimide aerogels, which consisted of a three-dimensional network of polyimide fibers tangled together. By varying the solution concentration of the polyimide containing trimethoxysilane side groups, polyimide aerogels with different densities (ranging from 0.19 to 0.42 g/cm^3) were obtained. The resulting polyimide aerogels had small pore diameter (ranging from 20.7 to 58.3 nm), high surface area (ranging from 310 to 344 m^2/g), high 5% weight loss temperature in air (at about 440 °C), and an excellent mechanical property. In addition, the glass transition temperature (349 °C) of the polyimide aerogels was much higher than that (210 °C) of the corresponding linear polyimide. So, even after being heated at 300 °C for 30 min, the porous structure of the polyimide aerogels was not completely destroyed.

INTRODUCTION

Aerogels are lightweight, open-celled, mesoporous materials prepared by replacing the fluids contained in gels by air without collapsing the pore structure.[1,2] Because of their many unique characteristics, such as low density, high porosity, low dielectric constant, low thermal conductivity, high surface area, and high acoustic impedance, aerogels have drawn great interest in a wide range of applications, including heat insulator, dust capturer for space applications, support for catalysts, low dielectric constant material for semiconductor devices, adsorbent, drug carrier, and sound attenuator.[3−7]

Among various aerogels, silica aerogel is the most well-known and extensively studied. However, the poor mechanical property greatly hinders its widespread application. For example, the collapse strengths under compression of pure silica aerogel with mass densities of 0.112 and 0.240 g/cm^3 are only 0.018 and 1.01 MPa, respectively.[8,9] The fragility of silica aerogel is traced to the weak interconnection in its "pearl-necklace-like" network structure, which is formed between secondary spherical silica particles held together.[10,11] To improve the mechanical property of silica aerogel, various strategies have been investigated, most notably via cross-linking of its skeletal framework with polymers.[7,12−17]

In addition to pure silica aerogel and reinforced silica aerogels, polymeric aerogels like syndiotactic polystyrene,[18] polyurethane,[19] polyurea,[20] cellulose,[1] poly(vinyl alcohol),[21] polyamide,[22] polybenzoxazine,[23] polyimide,[3,24−26] and chitin[27] have also been prepared. Compared with pure silica aerogel, polymeric aerogels possess better mechanical properties.[1,20,22,27,28]

Polyimide is an important high-performance material with good thermal stability, excellent mechanical property, and low dielectric constant, as well as outstanding chemical and radiation resistance. Some pioneering work on polyimide aerogel has been reported. Previously, linear polyimide aerogels were prepared by chemical imidization of poly(amic acid)s synthesized from dianhydrides and diamines in solvents, followed by supercritical drying.[29] During chemical imidization, the newly formed rigid polyimide chain segments caused the polymers to form gels because the rigid polyimides were insoluble and separated from the solvents. However, the completion of chemical imidization at room temperature was hindered by the increased immobility of polyimide's rigid structure. So polyimide aerogels prepared by the method required a thermal treatment to convert the residual amic acid group to the imide group. Furthermore, the thermal treatment was also needed to rearrange the instable isoimide group formed during chemical imidization to the imide group. The thermal treatment was performed either before or after supercritical drying of the polyimide gels. If the thermal treatment was carried out before the supercritical drying, the polyimide gels

should be put in a pressurized autoclave in order to reduce the solvent evaporating from the gels. If the thermal treatment was carried out after the supercritical drying, the heating rate should be slow enough to prevent shrinkage of the polyimide aerogels resulting from melting.

In 2010, Leventis and co-workers introduced an alternative route where linear polyimide aerogels were prepared by supercritical drying of polyimide gels synthesized from a dianhydride and a diisocyanate, eliminating the chemical imidization process.[30] But polyimide aerogel made by this way exhibited much weaker mechanical strength than chemically identical polyimide aerogel prepared from a dianhydride and a diamine. Then, Leventis et al. prepared cross-linked polyimide aerogels synthesized from dianhydrides and triisocyanates.[31] This kind of polyimide aerogel was very sturdy, indicating the strength of polymeric aerogels could be improved by introducing a cross-linked structure.

In 2011, Leventis and co-workers reported another kind of cross-linked polyimide aerogel, which was prepared by supercritical drying of polyimide gels synthesized from a norbornene end-capped diimide.[32] This kind of polyimide aerogel combined facile one-step synthesis with high mechanical strength and specific energy absorption. However, they had unsaturated backbone, which limited their use in air at high temperature.

In recent years, Meador and co-workers have fabricated cross-linked polyimide aerogels by reacting poly(amic acid) oligomers containing terminal anhydride groups with cross-linkers [either 1,3,5-triaminophenoxybenzene or octa(aminophenyl)-silsesquioxane] to produce cross-linked poly(amic acid) structures, followed by chemical imidization at room temperature and supercritical drying.[3,24−26] In 2012, the kind of polyimide aerogel fabricated by Meador and co-workers was recognized as one of the 100 most technologically significant products to enter the marketplace by the prestigious science journal *R&D*.[33] However, poly(amic acid) could not be completely imidized by chemical imidization reagents at room temperature, and instable isoimide group could be formed during chemical imidization.[29,30] Furthermore, the cross-linked poly(amic acid) gels made from the reaction of cross-linkers with short poly(amic acid) oligomers formed too quickly for incorporation of chemical imidization reagents.[25]

In this study, trimethoxysilanes were incorporated into every repeating unit of a polyimide as side groups, and the hydrolysis and condensation reactions of the trimethoxysilane contributed to the formation of highly cross-linked polyimide gels. Before gelation, the polyimide containing trimethoxysilane side groups was imidized completely via thermal imidization, eliminating the need for chemical imidization reagents and the problem of incomplete imidization. The polyimide gels were then dried by freeze-drying from *tert*-butyl alcohol to obtain polyimide aerogels, avoiding expensive and time-consuming supercritical drying. In addition, high mechanical strength and good thermal stability of the polyimide aerogels were achieved due to the highly cross-linked structure.

EXPERIMENTAL SECTION

Materials. 2,2-Bis[4-(3,4-dicarboxyphenoxy)phenyl]-propanedianhydride (BPADA) and 3,5-diaminobenzoic acid (DBA) were recrystallized from 9/1 acetic anhydride/toluene and water, respectively, before use. *N*,*N*′-Dimethylformamide (DMF) was distilled under vacuum over phosphorus pentoxide and stored over 4 Å molecular sieves. 3-Aminopropyltrimethoxysilane, *m*-cresol, triethylamine, thionyl chloride, and *tert*-butyl alcohol were guaranteed-grade and used as received.

Measurements. Proton-nuclear magnetic resonance (^{1}H NMR) spectra were performed on a Bruker AVANCE III 400 in dimethyl-d_6 sulfoxide at a resonance frequency of 400 MHz. Solid-state ^{29}Si nuclear magnetic resonance (^{29}Si NMR) spectrum was collected on a Bruker AVANCE III 400 spectrometer at a resonance frequency of 79.30 MHz. Inherent viscosity was measured with an Ubbelodhe viscometer at 30 ± 0.1 °C in DMF at a concentration of 0.5 g/dL. The rheological property was measured on a rotational Physica MCR 301 rheometer. The stain amplitude was set at 1%, and the sweep frequency was set at 1 Hz (well inside the linear viscoelastic range). Bulk density was calculated from weight and physical dimension of samples. The skeletal density was measured using a Micromeritics Accupyc 1340 helium pycnometer. The morphology was observed with a Hitachi TM-1000 scanning electron microscope (SEM). Before the SEM observation, the samples were sputter-coated with gold. Dynamic mechanical thermal analysis (DMTA) was conducted with a Mettler Toledo DMA in tensile mode at a heating rate of 5 °C/min and a frequency of 1 Hz. Thermogravimetric analysis (TGA) was performed under air atmosphere (flow rate of 50 mL/min) at a heating rate of 10 °C/min from 50 to 800 °C with a Mettler Toledo-TGA/DSC I instrument. The mechanical property was measured by an Instron model 5567 tensile tester at room temperature. The nitrogen adsorption−desorption measurement was carried out on a Micromeritics ASAP 2020 M system at the temperature of liquid nitrogen. Before measurement, all the samples were outgassed at 80 °C for 10 h. The surface area was determined from the adsorption curve by the Brunauer−Emmet−Teller method, and the pore size distribution was determined from the desorption curve by the Barret−Joyner−Halenda method.

Synthesis of Polyimide Containing Carboxylic Acid Side Groups. To a 100 mL three-necked round-bottomed flask equipped with a mechanical stirrer and a thermometer were added BPADA (10.4098 g, 20.0 mmol), DBA (2.9055 g, 19.1 mmol), and *m*-cresol (50 mL). The mixture was stirred at 200 °C for 8 h under nitrogen atmosphere to yield a viscous solution. After cooling to room temperature, the viscous solution was diluted with *m*-cresol and trickled into excess ethanol with stirring to afford a precipitate of polyimide containing carboxylic acid side groups. The precipitate was collected, washed thoroughly with hot ethanol, and dried under vacuum at 120 °C for 12 h. The polyimide containing carboxylic acid side groups had an inherent viscosity of 0.36 dL/g when measured in DMF at a concentration of 0.5 g/dL at 30 °C.

Synthesis of Polyimide Containing Trimethoxysilane Side Groups. To a 50 mL round-bottomed flask were added the polyimide containing carboxylic acid side groups (0.6366 g), $SOCl_2$ (5 mL), and two drops of DMF. The mixture was stirred at reflux temperature for 0.5 h. After removal of $SOCl_2$, 3-aminopropyltrimethoxysilane (0.1793 g, 1.0 mmol), triethylamine (0.1012 g, 1.0 mmol), and DMF (8 mL) were added. The reaction mixture was stirred at room temperature for 2 h and then filtered to remove precipitated triethylamine hydrochloride. The resulting DMF solution of polyimide containing trimethoxysilane side groups could be used in the next step directly without separation.

Preparation of Polyimide Aerogels. The preparation of sample 1 is used below as an example. To the obtained DMF solution of polyimide containing trimethoxysilane side groups was added a solution of water (0.0900 g, 5.0 mmol) and HCl (0.0073 g, 0.20 mmol) in DMF (12 mL). The reaction mixture was stirred vigorously for 3 min and then drawn into syringes. A gel was formed and aged in the syringes for 2 days at room temperature. After the aging treatment, the resulting gel was removed from the syringes. The solvent within the gel was exchanged with *tert*-butyl alcohol (four times at room temperature, 12 h each time, using about 10× the volume of the gel for each time). Finally, the gel containing *tert*-butyl alcohol was frozen and subjected to freeze-drying at −25 °C under vacuum. For polyimide aerogels with different densities, they were obtained by varying the concentration of polyimide containing trimethoxysilane side groups in DMF.

Scheme 1. Synthesis Route for Polyimide Containing Trimethoxysilane Side Groups

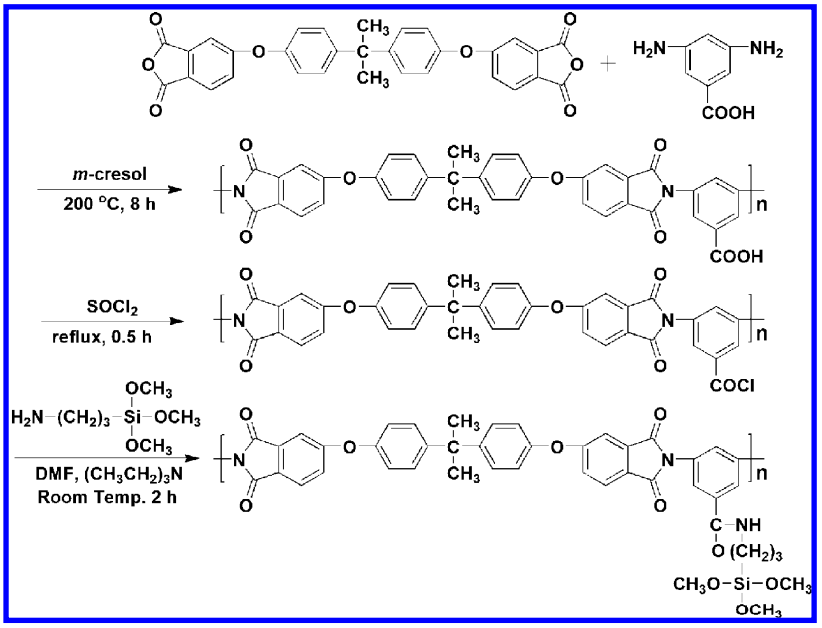

RESULTS AND DISCUSSION

In this study, polyimide gels with cross-linked Si–O–Si network structure were prepared through the hydrolysis and condensation reactions of trimethoxysilane side groups on the polyimide backbone. The polyimide containing trimethoxysilane side groups was synthesized according to a three-step procedure as shown in Scheme 1. First, polyimide containing carboxylic acid side groups was conveniently prepared by the polycondensation reaction of BPADA and DBA. Then, the carboxylic acid groups were converted into acid chloride groups, which were susceptible to react with the amino group of 3-aminopropyltrimethoxysilane.

The complete imidization of the polyimide containing carboxylic acid side groups was confirmed by ^{1}H NMR and FT-IR spectra. Figure S1 of the Supporting Information shows the ^{1}H NMR spectra of the polyimide containing carboxylic acid side groups and its intermediate poly(amic acid) containing carboxylic acid side groups, for which all the signals were assigned to the hydrogen atoms of the repeating units, as expected. After imidization, the ^{1}H NMR signal at 8.22 ppm corresponding to the amide group disappeared. Figure S2 of the Supporting Information shows the FT-IR spectra of the polyimide containing carboxylic acid side groups and its intermediate poly(amic acid) containing carboxylic acid side groups. The poly(amic acid) containing carboxylic acid side groups exhibited the characteristic amide group absorptions at 1655 cm^{-1} (C=O stretching) and 1560 cm^{-1} (C–NH stretching). After imidization, the characteristic absorption bands of the amide group disappeared and the polyimide containing carboxylic acid side groups exhibited the imide group absorptions at 1779 cm^{-1} (asym C=O stretching) and 1727 cm^{-1} (sym C=O stretching, including the C=O stretching of the carboxylic acid side groups).

The ^{1}H NMR spectrum of the polyimide containing trimethoxysilane side groups is shown in Figure S3 of the Supporting Information, in which all the signals were assigned as expected. After incorporating 3-aminopropyltrimethoxysilane, the ^{1}H NMR signal at 13.41 ppm corresponding to the proton of carboxylic acid side group on polyimide disappeared and the signal corresponding to amide linkage appeared at 8.59 ppm. On the basis of the results of ^{1}H NMR, the polyimide containing trimethoxysilane side groups was successfully synthesized in this study.

Scheme 2 presents the synthesis route for polyimide gel with the aid of trimethoxysilane side groups on polyimide. Methoxy groups on the silicon atom were hydrolyzed to hydroxyls that subsequently condensed with each other or with the methoxy groups on silicon atom to give rise to Si–O–Si bonds.[34,35] Since alkoxysilane hydrolysis is very slow under neutral conditions, hydrochloric acid was used as a catalyst.[34,35]

Gelation is a gradual transition from a viscoelastic liquid to a viscoelastic solid, and the measurement of the rheological property is particularly suitable to observe the gelation process and determine the gelation time.[36] Three polyimide aerogels with different densities were obtained by varying the concentration of polyimide containing trimethoxysilane side groups in DMF (Table 1). Figure 1a shows a continuous increase in the complex viscosities of the polyimide solutions with time at room temperature after adding water and acid catalyst, which indicated that a cross-linked Si–O–Si network structure formed and developed in the polyimide solutions as the hydrolysis and condensation reactions of trimethoxysilane side groups progressed. Figure 1b shows the evolution of the storage modulus G', which corresponds to the energy stored during deformation, and loss modulus G'', which corresponds to the energy dissipated during deformation with reaction time, for the three samples. In general, the crossover of G' and G'' as a function of time occurs near the gelation point and is taken as a sufficient approximation for the later.[36,37] According to the rule, the gelation point of samples 1, 2, and 3 were at about 4, 21, and 38 min, respectively. With increasing the concentration of polyimide containing trimethoxysilane side groups in DMF, the complex viscosity at the same reaction time increased and the gelation time decreased obviously. This was because the high content of trimethoxysilane side group contributed to faster formation of the cross-linked structure and higher cross-link density.

In order to strengthen the cross-link network, the polyimide gels were aged for 2 days before being removed from the mold.

Scheme 2. Synthesis Route for Cross-Linked Polyimide Gel with the Aid of Trimethoxysilane Side Groups

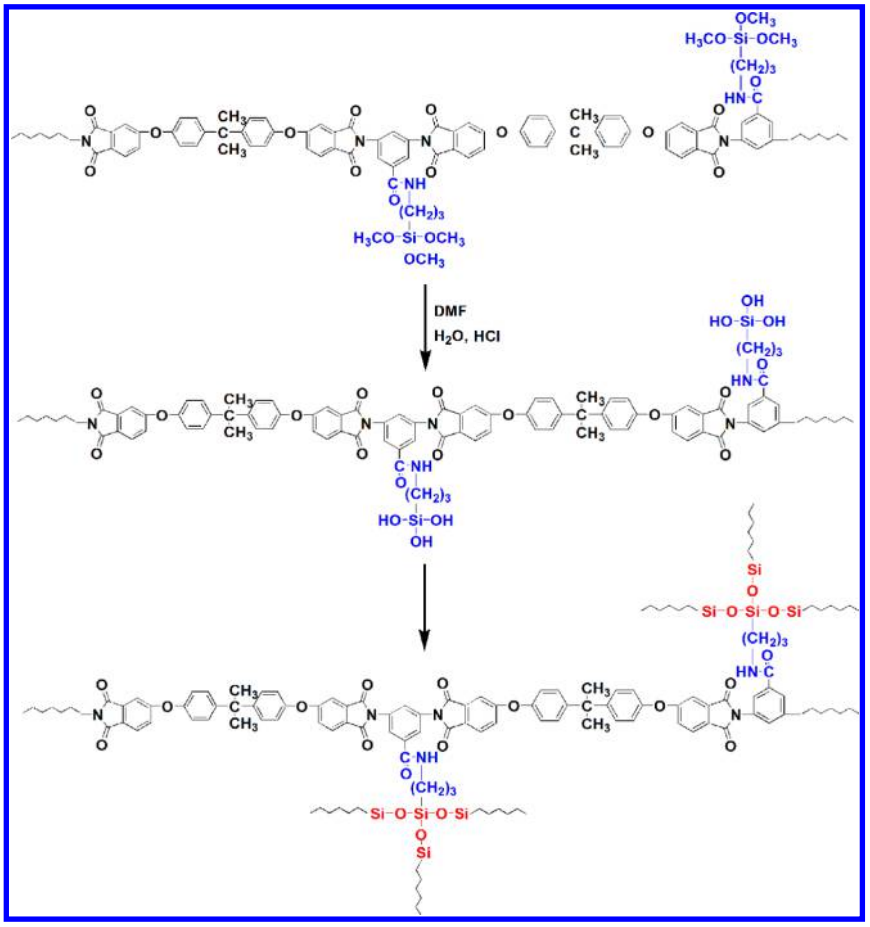

Table 1. Characterization Data of the Polyimide Aerogels

sample	solid content (g/mL)	density (g/cm^3)	shrinkage (%)[a] during aging	shrinkage (%)[a] during solvent exchange	shrinkage (%)[a] during freeze-drying	BET surface area (m^2/g)	porosity (%)[b]	V_{Total}[c] (cm^3/g)	average pore diameter[d] (nm)
1	0.04	0.19 ± 0.01	23	14	6	310	86	2.32 [4.52]	29.9 [58.3]
2	0.05	0.27 ± 0.01	29	10	5	331	80	2.38 [2.96]	28.8 [35.8]
3	0.06	0.42 ± 0.02	32	7	7	344	69	1.85 [1.78][e]	21.5 [20.7][e]

[a]Shrinkage was calculated via 100 × (mold diameter − sample diameter)/(mold diameter). [b]Porosity was calculated via 100 × $(1 - \rho_{bulk}/\rho_{skeletal})$, where ρ_{bulk} was the bulk density and $\rho_{skeletal}$ was the skeletal density. The $\rho_{skeletal}$ of the polyimide aerogels was 1.34 g/cm^3, as determined by means of a helium pycnometer. [c]V_{Total} was the total pore volume per gram of sample. For the first number, V_{Total} was calculated from the highest volume of nitrogen adsorbed along the adsorption isotherm; for the number in brackets, V_{Total} was calculated from the relationship $V_{Total} = (1/\rho_{bulk}) - (1/\rho_{skeletal})$. [d]The average pore diameter was determined by the $4V_{Total}/\sigma$ method, where σ was the surface area determined by the Brunauer–Emmet–Teller method. For the first number, V_{Total} was calculated from the highest volume of nitrogen adsorbed along the adsorption isotherm; for the number in brackets, V_{Total} was calculated from the relationship $V_{Total} = (1/\rho_{bulk}) - (1/\rho_{skeletal})$. [e]The density of sample 3 used for nitrogen adsorption–desorption measurement was 0.396 g/cm^3.

Figure 2 shows a gel of sample 1 as an example. During the aging, the cross-link reaction proceeded in the polyimide gel. As a result, the polyimide gel shrank and a portion of the solvent (DMF) was expelled from the polyimide gel. The resulting polyimide gels were elastic and strong. After solvent exchange with *tert*-butyl alcohol, they became hard and gray and lost transparency.

^{29}Si solid-state NMR was used to determine the condensation degree of the methoxy groups on silicon atom. The ^{29}Si solid-state NMR spectrum of sample 2 is shown in Figure S4 of the Supporting Information (Since the three polyimide aerogels with different densities had the same chemical structure, only the ^{29}Si solid-state NMR spectrum of sample 2 was measured). According to Loy et al. and Sugahara and co-workers, the signals between −40 and −75 ppm were assigned to three types of silicon.[38,39] In order to clarify the condensation degree of the methoxy groups on silicon atom, curve fitting and peak integration were carried out using the Fityk software. The molar ratio of $[-Si(OCH_3)_2(OSi)$, $-Si(OH)_2(OSi)$, and $-Si(OH)(OCH_3)(OSi)]$:$[-Si(OCH_3)(OSi)_2$ and $-Si(OH)(OSi)_2]$:$[-Si(OSi)_3]$ was 0.251:0.544:0.205, indicating that 65.1% of the methoxy groups on silicon atom formed a cross-linked siloxane network.

The polyimide containing trimethoxysiloxane side groups was soluble in DMF. However, if the aged polyimide wet gel

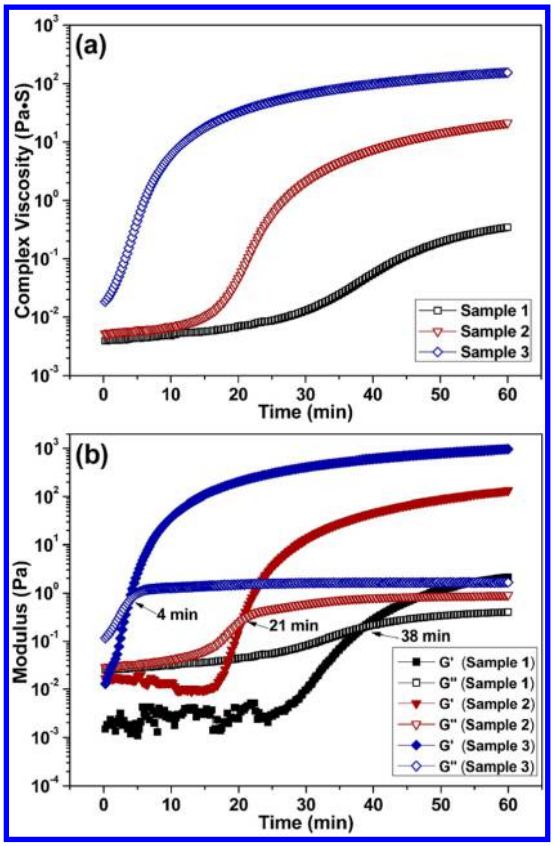

Figure 1. (a) Evolution of complex viscosity versus time from adding water and HCl in the DMF solution of polyimide containing trimethoxysilane side groups. (b) Evolution of storage modulus (G') and loss modulus (G'') versus time from adding water and HCl in the DMF solution of polyimide containing trimethoxysilane side groups.

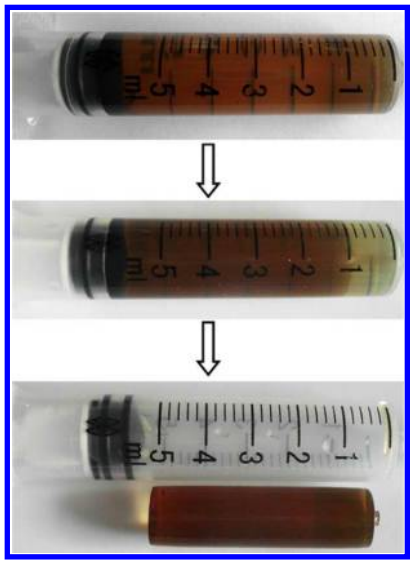

Figure 2. Photographs of sample 1 before aging (top), sample 1 after aging for 2 days (middle), and sample 1 removed from the syringe (bottom).

was kept in DMF for 1 day at 100 °C (the volume of DMF was 20× the volume of the wet gel), 95−98 wt % polyimide was still insoluble. According to Feulner et al., the degree of cross-linking could be calculated as the ratio of the mass of insoluble portion to the total mass of insoluble and soluble portions.[40] So the kind of polyimide aerogel had a high degree of cross-linking (ranging from 95 to 98%).

The gel is a three-dimensional porous structure filled with fluid. With the evaporation of fluid within a pore, capillary pressure begins to form.[7] Since the capillary pressure is inversely related to the pore size, the capillary pressure is very high for aerogel with nanometer-sized pores.[5] As a result, the ambient pressure drying method generally causes drastic shrinkage or cracking of the aerogel.[7] To prevent the damage to the aerogel structure, the drying process has to be done under special conditions.

Supercritical drying is the most commonly used method for gel drying. During supercritical drying, the phase boundary between the liquid phase and the vapor phase disappears and the fluid in pores can be removed without introducing the capillary pressure.[41] However, the supercritical drying is expensive and time-consuming.[42] Another method that could avoid the formation of capillary pressure in pores is freeze-drying, where the solvent in the gel is frozen and then removed by sublimation.[7] Before freeze-drying, the fluid in the gel should be exchanged with a solvent the density of which does not exhibit considerable change upon freezing. Otherwise, the expansion or shrinkage of solvent upon freezing could result in damage to the gel structure. *tert*-Butyl alcohol is a solvent for which the density change upon freezing is small.[43] Furthermore, it has a high sublimation pressure; thus, the time required for freeze-drying could be shortened.[43] So, in this study, the polyimide aerogels were freeze-dried from *tert*-butyl alcohol.

All of the polyimide aerogels shrank relative to the mold during fabrication. The shrinkages of the polyimide aerogels during fabrication ranged from 43 to 46%, measured as the difference between the diameter of the syringe and that of dried samples. In comparison with some previous reports about polyimide aerogels, the polyimide aerogels showed relatively high shrinkage.[25,30,32] In addition, the shrinkage of the polyimide aerogel increased with increasing the concentration of polyimide containing trimethoxysiloxane side groups in DMF. Shrinkage was reflected upon the bulk densities of the final polyimide aerogels. As a result, the density of the polyimide aerogels increased from 0.19 ± 0.01 to 0.42 ± 0.02 g/cm^3 with increasing the concentration of polyimide containing trimethoxysilxane side groups in DMF from 0.04 to 0.06 g/mL. As shown in Table 1, the shrinkage took place during aging, solvent exchange, and freeze-drying. Among these, the majority of shrinkage was observed during aging, resulting from the highly cross-linked network structure in the polyimide gels. It is interesting to note that the shrinkage during aging increased with increasing the concentration of polyimide containing trimethoxysilxane side groups in DMF, while the shrinkage during solvent exchange showed an inverse trend. This could be explained by the fact that the strength of polyimide gel prepared from a high concentration of polyimide containing trimethoxysilxane side groups was higher than that of polyimide gel prepared from a lower concentration of polyimide containing trimethoxysilxane side groups.

Figure 3 shows the morphological characteristics of the polyimide aerogels as a function of density using SEM. Unlike silica aerogel that is formed from aggregates of small particles with little visible interstitial porosity, the polyimide aerogels consisted of a three-dimensional network of polyimide fibers tangled together. This is similar to the morphology of some reported polyimide aerogels.[24−26,30] In addition, an increase in

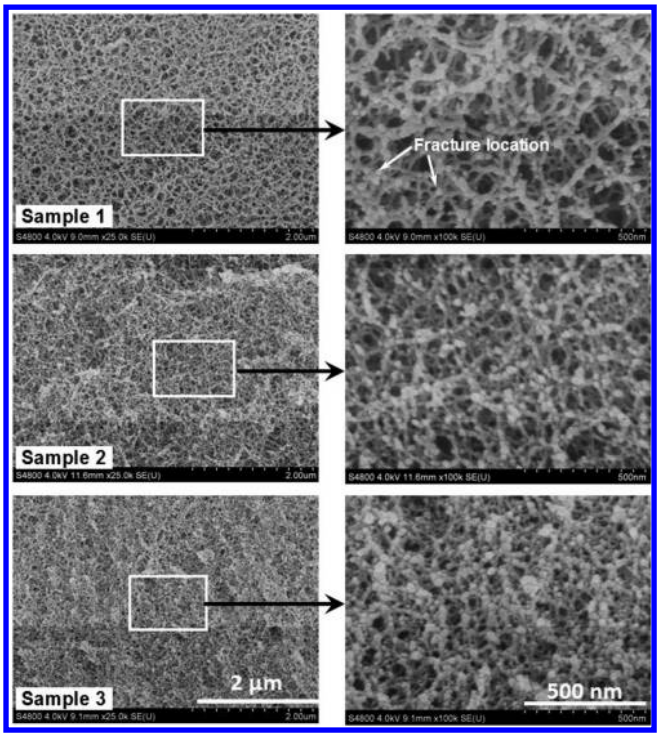

Figure 3. SEM images of the polyimide aerogels. Photos on the right are the enlargements of each area surrounded by a white line in the photos on the left.

the density of polyimide aerogels led to denser fibrillar structure and less pore size.

Pores are usually classified on the basis of their diameter (or width) as micropores (below 2 nm), mesopores (between 2 and 50 nm), and macropores (above 50 nm).[44] International Union of Pure and Applied Chemistry (IUPAC) has developed standards to classify gas adsorption–desorption isotherms and their relationship to the pore size of materials. Figure 4a shows the N_2 adsorption–desorption isotherms of the polyimide aerogels. According to the IUPAC classification, the N_2 adsorption–desorption isotherms of the polyimide aerogels were IUPAC type IV curves, indicating the presence of a significant fraction of mesopores. At high relative pressure ($P/P_o > 0.8$), the volume of N_2 adsorbed increased very quickly due to the capillary condensation in mesopores. Since the capillary condensation pressure tends to gradually decrease as the pore size decreases,[45,46] the onset of a quick increase in the volume of N_2 adsorbed moved to lower P/P_o value as the density of the polyimide aerogel increased. Furthermore, capillary condensation and capillary evaporation often do not take place at the same pressure, which led to the appearance of hysteresis loops.[45] The pore size distributions of the polyimide aerogels determined from their desorption curves by the Barret–Joyner–Halenda method are presented in Figure 4b. The sample with lower density showed broader pore size distribution and larger pore size. The average pore diameter in Table 1 was determined by the $4V_{Total}/\sigma$ method, where V_{Total} is the total pore volume per gram of sample and σ is the surface area determined by the Brunauer–Emmet–Teller (BET) method. The surface areas of the polyimide aerogels inferred from their adsorption curves by the BET method were in the range of 310–344 m^2/g. Probably because N_2 sorption did not probe large pores, the average pore diameter was lower when V_{Total} was calculated from the highest volume of nitrogen

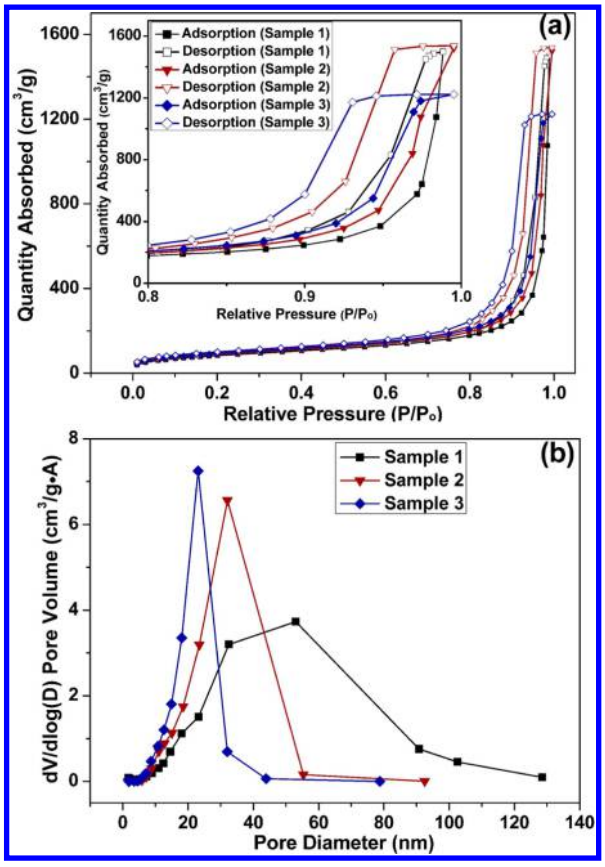

Figure 4. (a) N_2 adsorption–desorption isotherms of the polyimide aerogels. (b) Pore size distribution of the polyimide aerogels.

adsorbed along the adsorption isotherm than when V_{Total} was calculated from the relationship $V_{Total} = (1/\rho_{bulk}) - (1/\rho_{skeletal})$. In addition, when V_{Total} was calculated from the relationship $V_{Total} = (1/\rho_{bulk}) - (1/\rho_{skeletal})$, the average pore diameters agreed well with Figure 4b.

Figure 5a shows a picture of sample 1 (density of 0.20 g/cm^3, diameter of 12.0 mm, height of 7.5 mm), which can support a

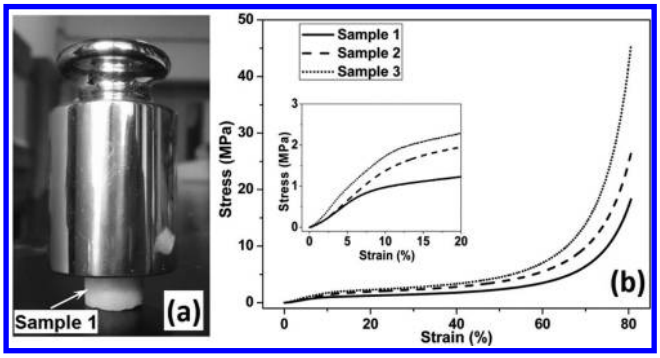

Figure 5. (a) Strength of the polyimide aerogels demonstated by supporting a 200 g weight with sample 1 (density of 0.20 g/cm^3, diameter of 12.0 mm, height of 7.5 mm). (b) Compressive stress–strain curves of the polyimide aerogels (inset: low-strain region magnified).

200 g weight without any deformation, indicating that the prepared polyimide aerogels were also robust. The stress–strain curves obtained from the compression test of the polyimide aerogels are shown in Figure 5b. They exhibited a short linear range at the initial stage of compression (<10%). Then, the

compressive stress increased slowly with increasing strain (in the range of 10−60%), in analogy to other polyimide and polymeric aerogels.[22,28,30,32] It was because, with increasing strain, the polyimide fibers were squeezed closer to one another and the pore size decreased. During the late stage of the compression test (>60%), the pores were substantially closed and the stress increased quickly. Different from pure silica aerogel, which shatters into many tiny fragments after compression, the polyimide aerogels remained in a single piece and turned into a dense solid after application of a large compressive load. Figure S5 of the Supporting Information shows the SEM micrograph of sample 2 after 80% compression strain as an example. In fact, except for linear polyimide aerogels prepared by supercritical drying of polyimide gels synthesized from a dianhydride and a diisocyanate, most of the polyimide aerogels have a good mechanical property.[25,30−32] Among them, the compressive stresses at about 80% strain of about 0.43 g/cm^3 cross-linked polyimide aerogels synthesized from dianhydrides and triisocyanates were above 100 MPa, which was more than twice the strength of the same density sample in the literature.[31]

The TGA curves under an air atmosphere of the polyimide aerogels are shown in Figure S6 of the Supporting Information. Their 5 wt % loss temperatures were in the range of 425−450 °C. After TGA measurement, about 7.5 wt % white degradation product was left. It was the trimethoxysilane side groups on polyimide that formed cross-linked Si−O−Si network structure in the polyimide aerogels after the hydrolysis and condensation reactions. If the trimethoxysilane side groups hydrolyzed and condensed completely, the weight percent of element silicon in the polyimide aerogels was 3.85 wt %. In addition, SiO_2 is the principal degradation product under an air atmosphere for siloxane-contained polymers.[47,48] For these reasons, the theoretical residue of SiO_2 was 8.24 wt %, which was close to the true value.

DMTA measurement of a dense polyimide film prepared from evaporating the DMF in polyimide gel slowly was carried out to monitor the effect of cross-linking on the thermomechanical property of the polyimide aerogels. It is known that the commercialized polyimide developed by General Electric Co. in 1986 under the trademark Ultem is synthesized from BPADA and *m*-phenylenediamine.[49] The prepared polyimide aerogels had the same backbone structure as Ultem. So, for comparison, the DMTA measurement of Ultem was also conducted.

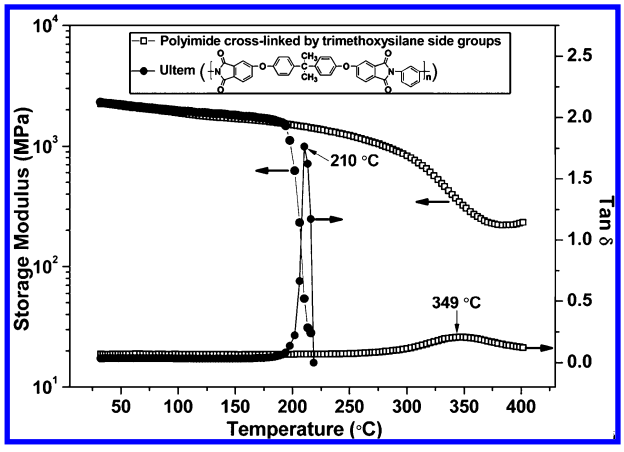

Figure 6. Storage modulus versus temperature curves and loss tangent (tan δ) versus temperature curves of the polyimide cross-linked by trimethoxysilane side groups and Ultem as determined by DMTA in air.

The storage modulus versus temperature curves and loss tangent (tan δ) versus temperature curves determined by DMTA are shown in Figure 6. The glass transition temperature (T_g) was identified by the peak temperature of the tan δ versus temperature curves. The T_g of Ultem was 210 °C, and there was a significant fall in its storage modulus on passing through the T_g, but for the polyimide cross-linked by trimethoxysilane side groups, the cross-linked structure enhanced its thermal stability. As a result, the polyimide cross-linked by trimethoxysilane side groups exhibited much higher storage modulus at high temperature and T_g (349 °C) than Ultem. The good thermal stability of polyimide cross-linked by trimethoxysilane side groups had a positive effect on the heat resistance of the polyimide aerogels. As shown in Figure 7, even after being heated at 300 °C for 30 min in air, the porous structure of sample 1 was not completely destroyed.

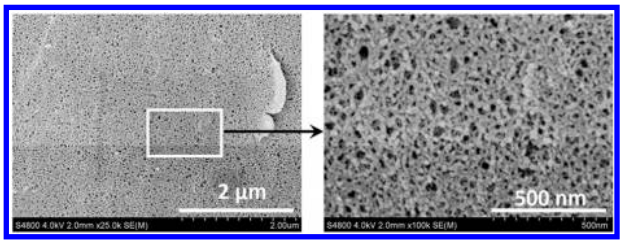

Figure 7. SEM image of sample 1 after being heated at 300 °C for 30 min in air. The photo on the right is an enlargement of the area surrounded by a white line in the photo on the left.

CONCLUSION

In this study, we introduced a new route to prepare polyimide aerogels. Trimethoxysilanes that could hydrolyze and condense one another to form the cross-linked Si−O−Si network structure were incorporated into the polyimide chain as side groups. The cross-linked structure was confirmed by rheology and ^{29}Si solid-state NMR to form and develop in the polyimide solution after adding water and acid catalyst. Although the polyimide aerogels showed high shrinkage (ranging from 43 to 46%) during fabrication, the majority of shrinkage was observed during aging, indicating the formation of a highly cross-linked network structure in the polyimide gel. The polyimide aerogels had high surface area, small pore size, and a good mechanical property, and the pore size could be tuned simply by adjusting the concentration of the polyimide containing trimethoxysilane side groups in DMF. The approach has significant advantages over previous approaches used to prepare polyimide aerogels. First, complete imidization of the polyimide aerogels was achieved by a thermal treatment before gelation, avoiding the need for chemical imidization reagents and the problem of incomplete imidization. Second, a high cross-linking degree of the polyimide aerogels was attained. Therefore, they exhibited high thermal stability.

ASSOCIATED CONTENT

Supporting Information

^{1}H NMR spectra of the polyimide containing carboxylic acid side groups and its intermediate poly(amic acid) containing carboxylic acid side groups (Figure S1), FT-IR spectra of the polyimide containing carboxylic acid side groups and its intermediate poly(amic acid) containing carboxylic acid side groups (Figure S2), ^{1}H NMR spectrum of polyimide containing trimethoxysilane side groups (Figure S3), ^{29}Si solid-state NMR

spectrum of sample 1 (Figure S4), SEM image of sample 2 after 80% compression strain (Figure S5), and TGA curves of the polyimide aerogels at a heating rate of 10 °C/min in air (Figure S6). This material is available free of charge via the Internet at http://pubs.acs.org.

AUTHOR INFORMATION

Corresponding Author

*E-mail: wgzheng@nimte.ac.cn.

Notes

The authors declare no competing financial interest.

ACKNOWLEDGMENTS

This work was financially supported by National Natural Science Foundation of China (Grant No. 51403226), Natural Science Foundation of Ningbo City, China (Grant No. 2014A610139), Guangdong-CAS Strategic Cooperation Project (Grant No. 2012B090400022), and National High Technology Research and Development Program of China (863 Program, Grant No. 2013AA032003).

REFERENCES

(1) Tan, C.; Fung, B. M.; Newman, J. K.; Vu, C. Organic Aerogels with Very High Impact Strength. *Adv. Mater.* **2001**, *13*, 644−646.

(2) Hegde, N. D.; Rao, A. V. Organic Modification of TEOS Based Silica Aerogels Using Hexadecyltrimethoxysilane as a Hydrophobic Reagent. *Appl. Surf. Sci.* **2006**, *253*, 1566−1572.

(3) Meador, M. A. B.; McMillon, E.; Sandberg, A.; Barrios, E.; Wilmoth, N. G.; Mueller, C. H.; Miranda, F. A. Dielectric and Other Properties of Polyimide Aerogels Containing Fluorinated Blocks. *ACS Appl. Mater. Interfaces* **2014**, *6*, 6062−6068.

(4) Katsoulidis, A. P.; He, J. Q.; Kanatzidis, M. G. Functional Monolithic Polymeric Organic Framework Aerogel as Reducing and Hosting Media for Ag Nanoparticles and Application in Capturing of Iodine Vapors. *Chem. Mater.* **2012**, *24*, 1937−1943.

(5) Smith, D. M.; Maskara, A.; Boes, U. Aerogel-Based Thermal Insulation. *J. Sol-Gel. Sci. Technol.* **1998**, *225*, 254−259.

(6) Sun, H. Y.; Xu, Z.; Gao, C. Multifunctional, Ultra-Flyweight, Synergistically Assembled Carbon Aerogels. *Adv. Mater.* **2013**, *25*, 2554−2560.

(7) Hüsing, N.; Schubert, U. Aerogels—Airy Materials: Chemistry, Structure, and Properties. *Angew. Chem., Int. Ed.* **1998**, *37*, 22−45.

(8) Deng, Z. S.; Wang, J.; Wu, A. M.; Shen, J.; Zhou, B. High Strength SiO_2 Aerogel Insulation. *J. Non-Cryst. Solids* **1998**, *225*, 101−104.

(9) Parmenter, K. E.; Milstein, F. Mechanical Properties of Silica Aerogels. *J. Non-Cryst. Solids* **1998**, *223*, 179−189.

(10) Zhang, G.; Dass, A.; Rawashdeh, A. M.; Thomas, J.; Counsil, J. A.; Sotiriou-Leventis, C.; Fabrizio, E. F.; Ilhan, F.; Vassilaras, P.; Scheiman, D. A.; McCorkle, L.; Palczer, A.; Johnston, J. C.; Meador, M. A.; Leventis, N. Isocyanate-Crosslinked Silica Aerogel Monoliths: Preparation and Characterization. *J. Non-Cryst. Solids* **2004**, *350*, 152−164.

(11) Woignier, T.; Phalippou, J. Mechanical Strength of Silica Aerogels. *J. Non-Cryst. Solids* **1988**, *100*, 404−408.

(12) Meador, M. A. B.; Weber, A. S.; Hindi, A.; Naumenko, M.; McCorkle, L.; Quade, D.; Vivod, S. L.; Gould, G. L.; White, S.; Deshpande, K. Structure Property Relationships in Porous 3D Nanostructures: Epoxy-Cross-Linked Silica Aerogels Produced Using Ethanol as the Solvent. *ACS Appl. Mater. Interfaces* **2009**, *1*, 894−906.

(13) Duan, Y. N.; Jana, S. C.; Lama, B.; Espe, M. P. Reinforcement of Silica Aerogels Using Silane-End-Capped Polyurethanes. *Langmuir* **2013**, *29*, 6156−6165.

(14) Yang, X. G.; Sun, Y. T.; Shi, D. Q.; Liu, J. L. Experimental Investigation on Mechanical Properties of a Fiber-Reinforced Silica Aerogel Composite. *Mat. Sci. Eng. A-Struct.* **2011**, *528*, 4830−4836.

(15) Mohite, D. P.; Larimore, Z. J.; Lu, H.; Mang, J. T.; Sotiriou-Leventis, C.; Leventis, N. Monolithic Hierarchical Fractal Assemblies of Silica Nanoparticles Cross-Linked with Polynorbornene via ROMP: A Structure−Property Correlation from Molecular to Bulk through Nano. *Chem. Mater.* **2012**, *24*, 3434−3448.

(16) Leventis, N. Three Dimensional Core−Shell Superstructures: Mechanically Strong Aerogels. *Acc. Chem. Res.* **2007**, *40*, 874−884.

(17) Leventis, N.; Sotiriou-Leventis, C.; Zhang, G.; Rawashdeh, A. M. M. Nano Engineering Strong Silica Aerogels. *Nano Lett.* **2002**, *2*, 957−960.

(18) Wang, X.; Jana, S. C. Tailoring of Morphology and Surface Properties of Syndiotactic Polystyrene Aerogels. *Langmuir* **2013**, *29*, 5589−5598.

(19) Chidambareswarapattar, C.; McCarver, P. M.; Luo, H.; Lu, H.; Sotiriou-Leventis, C.; Leventis, N. Fractal Multiscale Nanoporous Polyurethanes: Flexible to Extremely Rigid Aerogels from Multifunctional Small Molecules. *Chem. Mater.* **2013**, *25*, 3205−3224.

(20) Leventis, N.; Sotiriou-Leventis, C.; Chandrasekaran, N.; Mulik, S.; Larimore, Z. J.; Lu, H. B.; Churn, G.; Mang, J. Multifunctional Polyurea Aerogels from Isocyanates and Water. A Structure−Property Case Study. *Chem. Mater.* **2010**, *22*, 6692−6710.

(21) Chen, H. B.; Hollinger, E.; Wang, Y. Z.; Schiraldi, D. A. Facile Fabrication of Poly(vinyl alcohol) Gels and Derivative Aerogels. *Polymer* **2014**, *55*, 380−384.

(22) Leventis, N.; Chidambareswarapattar, C.; Mohite, D. P.; Larimore, Z. J.; Lu, H. B.; Sotiriou-Leventis, C. Multifunctional Porous Aramids (Aerogels) by Efficient Reaction of Carboxylic Acids and Isocyanates. *J. Mater. Chem.* **2011**, *21*, 11981−11986.

(23) Mahadik-Khanolkar, S.; Donthula, S.; Sotiriou-Leventis, C.; Leventis, N. Polybenzoxazine Aerogels. 1. High-Yield Room-Temperature Acid-Catalyzed Synthesis of Robust Monoliths, Oxidative Aromatization, and Conversion to Microporous Carbons. *Chem. Mater.* **2014**, *26*, 1303−1317.

(24) Guo, H. Q.; Meador, M. A. B.; McCorkle, L.; Quade, D. J.; Guo, J.; Hamilton, B.; Cakmak, C.; Sprowl, G. Polyimide Aerogels Cross-Linked through Amine Functionalized Polyoligomeric Silsesquioxane. *ACS Appl. Mater. Interfaces* **2011**, *3*, 546−552.

(25) Meador, M. A. B.; Malow, E. J.; Silva, R.; Wright, S.; Quade, D.; Vivod, S. L.; Guo, H. Q.; Guo, J.; Cakmak, M. Mechanically Strong, Flexible Polyimide Aerogels Cross-Linked with Aromatic Triamine. *ACS Appl. Mater. Interfaces* **2012**, *4*, 536−544.

(26) Guo, H. Q.; Meador, M. A. B.; McCorkle, L.; Quade, D. J.; Guo, J.; Hamilton, B.; Cakmak, M. Tailoring Properties of Cross-Linked Polyimide Aerogels for Better Moisture Resistance, Flexibility, and Strength. *ACS Appl. Mater. Interfaces* **2012**, *4*, 5422−5429.

(27) Ding, B. B.; Cai, J.; Huang, J. C.; Zhang, L. N.; Chen, Y.; Shi, X. W.; Du, Y. M.; Kuga, S. Facile Preparation of Robust and Biocompatible Chitin Aerogels. *J. Mater. Chem.* **2012**, *22*, 5801−5809.

(28) Yang, J.; Li, S. K.; Yan, L. L.; Liu, J. X.; Wang, F. C. Compressive Behaviors and Morphological Changes of Resorcinol−Formaldehyde Aerogel at High Strain Rates. *Micropor. Mesopor. Mat.* **2010**, *133*, 134−140.

(29) Rhine,W.; Wang, J.; Begag, R. Polyimide Aerogels, Carbon Aerogels, and Metal Carbide Aerogels and Methods of Making Same. U.S. Patent 7074880, 2006.

(30) Chidambareswarapattar, C.; Larimore, Z.; Sotiriou-Leventis, C.; Mang, J. T.; Leventis, N. One-Step Room-Temperature Synthesis of Fibrous Polyimide Aerogels from Anhydrides and Isocyanates and Conversion to Isomorphic Carbons. *J. Mater. Chem.* **2010**, *20*, 9666−9678.

(31) Chidambareswarapattar, C.; Xu, L.; Sotiriou-Leventis, C.; Leventis, N. Robust Monolithic Multiscale Nanoporous Polyimides and Conversion to Isomorphic Carbons. *RSC Adv.* **2013**, *3*, 26459−26469.

(32) Leventis, N.; Sotiriou-Leventis, C.; Mohite, D. P.; Larimore, Z. J.; Mang, J. T.; Churu, G.; Lu, H. B. Polyimide Aerogels by Ring-Opening Metathesis Polymerization (ROMP). *Chem. Mater.* **2011**, *23*, 2250−2261.

(33) 2012 R&D 100 Winner. http://www.rdmag.com/articles/2012/06/2012-r-d-100-award-winners?cmpid=related_content, accessed Aug 21, 2012.
(34) Loyt, D. A.; Shea, K. J. Bridged Polysilsesquioxanes. Highly Porous Hybrid Organic–Inorganic Materials. *Chem. Rev.* **1995**, *95*, 1431–1442.
(35) Ni, H.; Skaja, A. D.; Soucek, M. D. Acid-Catalyzed Moisture-Curing Polyurea/Polysiloxane Ceramer Coatings. *Prog. Org. Coat.* **2000**, *40*, 175–184.
(36) Job, N.; Panariello, F.; Crine, M.; Pirard, J. P.; Leonard, A. Rheological Determination of the Sol–Gel Transition During the Aqueous Synthesis of Resorcinol–Formaldehyde Resins. *Colloid. Surface. A* **2007**, *293*, 224–228.
(37) Zhang, J.; Cao, Y. W.; Feng, J. C.; Wu, P. Y. Graphene-Oxide-Sheet-Induced Gelation of Cellulose and Promoted Mechanical Properties of Composite Aerogels. *J. Phys. Chem. C* **2012**, *116*, 8063–8068.
(38) Loy, D. A.; Jamison, G. M.; Baugher, B. M.; Russick, E. M.; Assink, R. A.; Prabakar, S.; Shea, K. J. Alkylene-Bridged Polysilsesquioxane Aerogels: Highly Porous Hybrid Organic–Inorganic Materials. *J. Non-Cryst. Solids* **1995**, *186*, 44–53.
(39) Komori, Y.; Nakashima, H.; Hayashi, S.; Sugahara, Y. Silicon-29 Cross-Polarization/Magic-Angle-Spinning NMR Study of Inorganic–Organic Hybrids: Homogeneity of Sol–Gel Derived Hybrid Gels. *J. Non-Cryst. Solids* **2005**, *351*, 97–103.
(40) Feulner, R.; Brocka, Z.; Seefried, A.; Kobes, M.O.; Hülder, G.; Osswald, T.A. The Effects of E-Beam Irradiation Induced Cross Linking on the Friction and Wear of Polyamide 66 in Sliding Contact. *Wear* **2010**, *268*, 905–910.
(41) Lee, J. K.; Gould, G. L. Polydicyclopentadiene Based Aaerogel: A New Insulation Material. *J. Sol–Gel Sci. Technol.* **2007**, *44*, 29–40.
(42) Lu, A. H.; Li, W. C.; Schmidt, W.; Schüth, F. Fabrication of Hierarchically Structured Carbon Monoliths via Self-Binding and Salt Templating. *Micropor. Mesopor. Mat.* **2006**, *95*, 187–192.
(43) Tamon, H.; Ishizaka, H.; Yamamoto, T.; Suzuki, T. Preparation of Mesoporous Carbon by Freeze Drying. *Carbon* **1999**, *37*, 2049–2055.
(44) Sing, K. S. W.; Everett, D. H.; Haul, R. A. W.; Moscou, L.; Pierotti, R. A.; Rouquerol, J.; Siemieniewska, T. Reporting Physisorption Data for Gas/Solid Systems—With Special Reference to the Determination of Surface Area and Porosity. *Pure Appl. Chem.* **1985**, *57*, 603–619.
(45) Kruk, M.; Jaroniec, M. Gas Adsorption Characterization of Ordered Organic Inorganic Nanocomposite Materials. *Chem. Mater.* **2001**, *13*, 3169–3183.
(46) Kruk, M.; Jaroniec, M. Determination of Mesopore Size Distributions from Argon Adsorption Data at 77 K. *J. Phys. Chem. B* **2002**, *106*, 4732–4739.
(47) Ghosh, A.; Banerjee, S. Structure–Property Co-Relationship of Fluorinated Poly(imide-siloxane)s. *Polym. Adv. Technol.* **2008**, *19*, 1486–1494.
(48) McGrath, J. E.; Dunson, D. L.; Mecham, S. J.; Hedrick, J. L. Synthesis and Characterization of Segmented Polyimide–Polyorganosiloxane Copolymers. *Adv. Polym. Sci.* **1999**, *140*, 61–105.
(49) Xia, J. Z.; Liu, S. L.; Pallathadka, P. K.; Chng, M. L.; Chung, T. S. Structural Determination of Extem XH 1015 and Its Gas Permeability Comparison with Polysulfone and Ultem via Molecular Simulation. *Ind. Eng. Chem. Res.* **2010**, *49*, 12014–12021.